Flow Structure Generated by Oscillating Delta-Wing Segments

Thomas Utsch* and Donald Rockwell†
Lehigh University, Bethlehem, Pennsylvania

I. Introduction

USE of leading-edge flaps to improve the performance of aircraft with swept wings is a topic of considerable current interest, evidenced by the assessments of Lamar,[1] Lamar and Campbell,[2] and Rao.[3-5] Cavity flaps may be used to attain and control a range of maneuvers at high angle of attack. A wide variety of flap configurations exist, and a complete understanding of the underlying flow physics would be helpful in optimizing the flap design. Knowledge of the flow structure during unsteady wing motion is essential in predicting the features of the wing loading.

The deployment of leading-edge flaps may be related to the concept of the "clap and fling" employed by various insects in hovering flight (Weiss and Fogh[6]); both generate pronounced leading-edge vortices. Maxworthy[7] and Spedding and Maxworthy[8] have quantitatively described the clap and fling mechanism in the absence of mean flow in the axial direction. Spedding et al.[9] have demonstrated the generation of circulation due to flow past a swept leading-edge flap oscillating on a stationary half-wing.

The overall objective of this investigation is to characterize features of the unsteady flow structure past symmetrical delta-wing segments forced to oscillate about a common axis. In doing so, a new flow visualization technique is employed, involving laser-induced reflection from a grid of hydrogen bubbles.

II. Experimental Systems and Techniques

Figure 1 gives an overview of the symmetrical delta-wing segments and a simplified illustration of the concentric drive system. Each of the wing segments was connected through this drive train to two independent, computer-controlled stepping motors, allowing arbitrary forcing of each wing. Complete details of the forcing system are given by Utsch.[10]

Space limitations do not allow description of all of the geometrical and flow parameters (Utsch[10]). The Reynolds number $Re \equiv U_\infty C/\nu$ and reduced frequency $K \equiv \pi fC/U_\infty$ were in the ranges $10^4 \leq Re < 3.4 \times 10^4$ and $0.32 \leq K \leq 3.58$.

The flow structure was visualized by placing the hydrogen bubble (marker) in the grid generator, which produced continuous bubble sheets intersecting in an "egg crate" configuration. This system of intersecting bubble sheets was undistorted at its location of generation upstream of the wing system. When this bubble grid encountered the wing, it indicated the three-dimensional distortion of the flow structure. The plane of interest in the flow was illuminated by a laser sheet, produced by reflection from a mirror scanning at 500 cycles/s. The laser sheet could be translated in the direction of the freestream in order to allow examination of a desired cross section of the flow structure. End view images (looking upstream) were recorded on a video system that recorded 120 frames/s. By tracking the nodes of the grid, it was possible to determine the quantitative features of the unsteady flowfield.

A Zenith 241 computer drove each of the two stepping motors, which controlled the wing motion. It allowed generation of arbitrary sinusoidal motion and phase between them. The hydrogen bubble grid marker could be controlled either independently by a microprocessor controller or by the computer in order to allow arbitrary generation of bubble markers with prescribed frequency and duration.

III. Flow Structure at Zero Angle of Attack

If the symmetrical wing segments shown in Fig. 2 are oscillated in harmonic motion such that each wing segment is π out-of-phase with its neighbor, then the motion corresponds to a harmonic version of the clap and fling maneuver discussed in the Introduction. Stationary wing segments, oriented at zero mean angle of attack, i.e., $\alpha = 0$, do not induce formation of leading-edge vortices. When the wing segments are oscillated at sufficiently high reduced frequency $K = \pi fC/U$, vortex formation occurs from the leading edges of the wings.

Complete time series of the flow structure during the clap and fling portions of the oscillation cycle are given by Utsch.[10] Figure 2 shows representative excerpts from the clap portion of the oscillation cycle (Fig. 2a) and the fling portion of the cycle (Fig. 2b). The cross-stream velocity field can be determined by measuring changes in the distortion of the grid of bubbles shown in Fig. 2 over an incremental streamwise distance Δx. Each of the sets of photos in Fig. 2 represents the grid distortions at two different axial (x) locations and two instants of time $\Delta x/U_\infty$ where Δx is the distance between the images at $xC = 0.7$ and 0.8 and U_∞ is the freestream velocity. Complete details for determining the velocity field using this technique are given in detail by Utsch.[10] They include consideration of the instantaneous velocity field in the streamwise direction, which can be deduced using the technique illustrated in Fig. 3. In this case, the grid of bubbles corresponds to parallel, nonintersection horizontal sheets generated upstream of the delta-wing configuration. The bubble grid has a sharp leading edge, resulting from abruptly turning on the pulse generator. Figure 3 shows the encounter of the sharp front of this bubble grid with the thin (3-mm-thick) plane of laser light, while the wings oscillate in the harmonic clap and fling mode. The leading edge of the bubble encounters the laser sheet at different times, thereby producing a sequential "filling in" of the image shown for successive times in Fig. 3. The technique for deter-

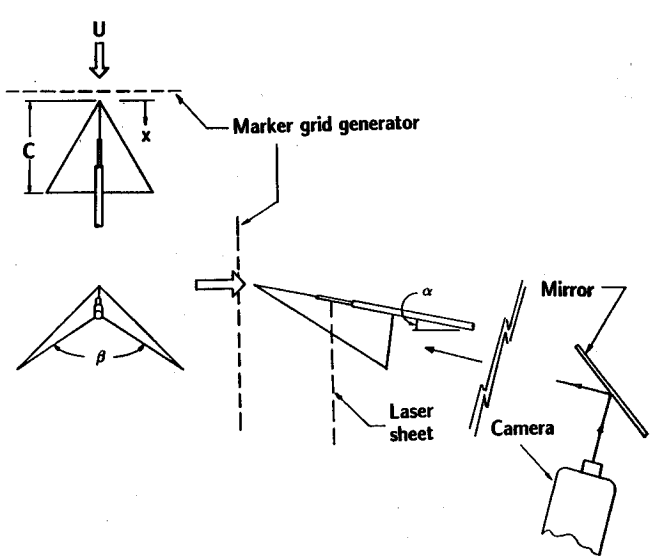

Fig. 1 Schematic of experimental system showing oscillation of delta-wing segments about common axis and deployment of camera and mirror arrangement in conjunction with translating laser sheet to obtain instantaneous images of flow structure. (Distance between trailing edge of wing and mirror is substantially longer than that shown.)

Received Sept. 6, 1988; revision received May 15, 1989.

*Lieutenant, U. S. Air Force
†Paul B. Reinhold Professor. Department of Mechanical Engineering. Member AIAA

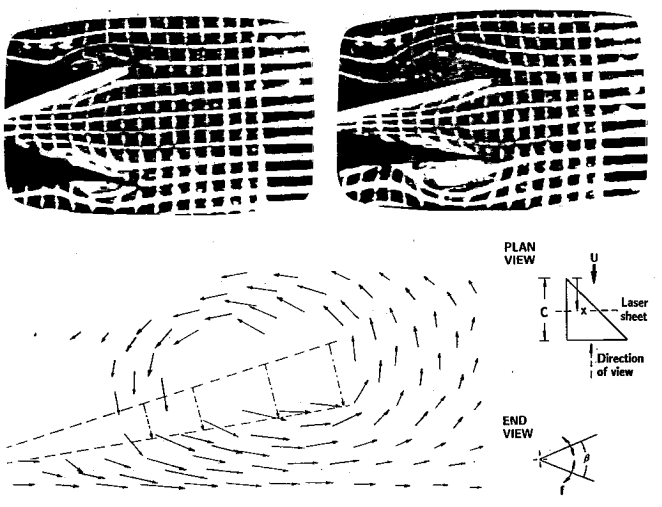

a)

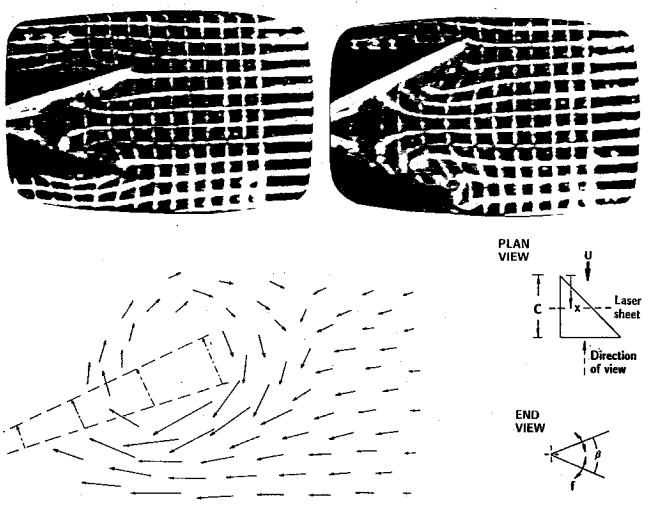

b)

Fig. 2 End view of delta-wing segments oscillating about common axis in harmonic version of clap and fling maneuver, with left photo taken at $x/C=0.7$ and right photo at $x/C=0.8$. Time delay between photos corresponds to travel time of bubbles moving at freestream velocity between $x/C=0.7$ and 0.8. (Bubble sheets have thickness of 100 μ, greatly exaggerated here due to video gain.) Velocity field of upper half of symmetric flow is obtained by tracking nodes of hydrogen bubble grid in preceding photos. Dashed lines shown movement of wing during time interval. $K=\pi fC/U_\infty=2.56$, $\beta_{max}=60$ deg, $\beta_{min}=15$ deg.

mining the axial velocity relative to the freestream is defined by Utsch.[10]

The resultant cross-stream velocity fields corresponding to the representative clap and fling motions in Fig. 2 are illustrated beneath each set of photographs. The circulation was evaluated by employing two integration circuits covering different-sized areas. The value of the dimensionless circulation for the flow pattern at the top of Fig. 2 is found to be $\Gamma^*=\Gamma/\dot{\theta}_m S_*^2=0.995$ and 0.987, suggesting that nearly all the vorticity in the vortex is concentrated within the inner circuit. In this definition of Γ^*, $\dot{\theta}_m$ is the maximum angular velocity of the wing segment and S_* is the semispan at the average x location (streamwise) over the interval Δt. Correspondingly, the value of dimensionless circulation over the fling portion of the maneuver represented by the bottom set of photographs in Fig. 2 is $\Gamma^*=0.77$. We therefore conclude that it is possible to generate the same order of magnitude of dimensionless circulation during the clap and fling portions of the maneuver.

An overview of the flow structure at the terminal stage of the clap (closing) of the wing segments is given in Fig. 4 for three values of reduced frequency at a location near the trailing edge of the wing, i.e., $x/C=0.95$. It is evident that the scale of the vortical motion is strongly dependent upon the reduced frequency K. At the highest value of $K=2.57$, the substantial value of dimensionless circulation $\Gamma^*=0.726$ of the vortex (about the upper wing segment) at this closed position of the wing segments emphasizes the importance of accounting for the phase shift between the wing motion and the vortex formation, as well as for the fact that the vortex is made up of vorticity shed from the upstream portions of the leading edge. That is, the azimuthal velocity of the edges of the wing is zero when the included angle $\beta=0$, yet the circulation Γ^* has a value close to that occurring when the wing has its maximum tangential velocity, as addressed Fig. 2. The evolution of these vortical patterns along the chord of the wing and the importance of accounting for the local span of the wing in defining the reduced frequency and the scale of the vortices are discussed by Utsch.[10]

IV. Flow Structure at Angle of Attack

When the wing segment arrangment of Fig. 1 is inclined at an angle of attack α with respect to the freestream, a small-scale leading-edge vortex exists in the absence of wing motion. The visualization of Fig. 5 shows the case where the mean angle $\bar{\beta}$ between the wings is 180 deg and each wing oscillates through a total angle of 60 deg (30 deg above and 30 deg below

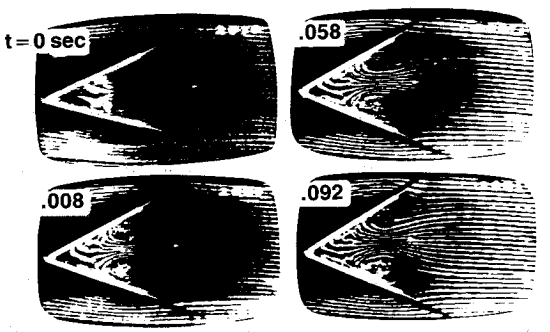

Fig. 3 Encounter of grid of horizontal bubble lines having discontinuous front with wing segments undergoing harmonic version of clap and fling maneuver. Filling in, or increasing glow intensity, is due to different times of arrival at stationary laser sheet of different portions of discontinuous grid of bubbles. At completion of filling in of image ($t=0.142$ s), $\beta=55$ deg. (Bubble sheets have a thickness of 100 μ, greatly exaggerated here due to video gain.) $\beta_{max}=60$ deg, $\beta_{min}=10$ deg, $K=(\pi fC)/U=3.6$, $x/C=0.6$. (See Fig. 2 for definition of x and β.)

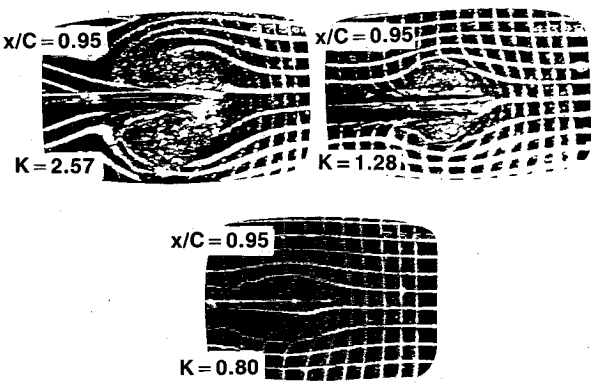

Fig. 4 View of delta-wing segments and vortex structure at termination of clap portion of harmonic version of clap and fling maneuver. (Bubble lines have thickness of 100 μ, greatly exaggerated due to video gain.) $\beta_{max}=30$ deg, $\beta_{min}=0$ deg. See Fig. 2 for definition of x and β.

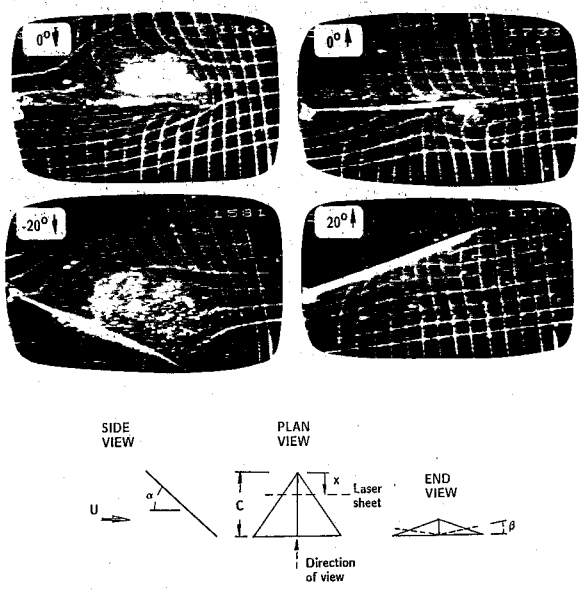

Fig. 5 End view of delta-wing segment undergoing harmonic oscillations. Their common axis is at static angle of attack with respect to freestream. Downward arrows ↓ correspond to downstroke of wing segment and upward arrows ↑ to upstroke. (Bubble sheets have thickness of 100 μ, greatly exaggerated here due to video gain.) $\alpha = 15$ deg, $\beta_{max} = +30$ deg, $\beta_{min} = -30$ deg, $K = (\pi fC)/U = 3.6$, $x/C = 1.06$, $x/C = 0.95$.

the horizontal reference line) as indicated schematically in Fig. 5. During the downstroke motion at $\beta = 0$ and -20 deg↓, there exists a large-scale vortical region on the upper surface of the wing. In contrast, during the corresponding upstroke motion at $\theta = 0$ and 20 deg↑, there is no discernible vortex formation. (A complete time sequence of this maneuver is given by Utsch.[10]) Reasoning on a quasisteady basis, it is possible to explain the qualitative difference between the flow structure during the upstroke and downstroke. During the downstroke, the angle of attack induced by the wing motion adds to the stationary angle of attack against the vortex formation. On the other hand, during the upstroke, the stationary angle of attack opposes the angle of attack induced by the wing motion.

Flow patterns for other configurations and angles of attack of the wing system are given by Utsch.[10] Evaluation of the instantaneous velocity field and circulation of the case of one segmented wing segment oscillating in the presence of an adjacent stationary segment oriented at angle of attack $\alpha = 15$ deg, with $\beta_{max} = 60$ deg and $\beta_{min} = 0$ deg, and $K = 0.48$, gives values of dimensionless circulation as high as $\alpha = 0$, $\Gamma^* = 0.99$, and 0.77 at $K = 2.56$ (see Fig. 2), it is evident that the effect of small angle of attack ($\alpha = 15$ deg) is to allow generation of higher values of circulation at substantially lower values of reduced frequency.

V. Conclusions

The well-known clap and fling mechanism involves transient, ramp-like movement of unswept wings about a common axis in a quiescent fluid, i.e., with no axial flow component. With the eventual aim of controlling the maneuverability of swept-wing aircraft, we have addressed here the complex situation of wing segments having swept leading edges, undergoing a harmonic version of the clap and fling mechanism in the presence of axial flow. In contrast to the purely two-dimensional wing oscillation in a quiescent fluid, the structure of the vortex in the present case is made up of vorticity shed from upstream regions of the leading edge of the wing. Consequently the circulation at any streamwise location will be a function of the upstream history of the flow.

At zero angle of attack, it is possible to attain substantial values of circulation $\Gamma^* \sim 1$, which is of the same order as that attained in the classical two-dimensional clap and fling. Regarding the comparison of circulation Γ^* generated during the clap and fling portions of the oscillation cycle, they are of the same order of magnitude. For both the clap and fling motions, the irrotational flow near the midplane of the interior of the wing segments is in a direction that promotes vortex formation.

The importance of considering the phase shift between the wing motion and the generation of circulation of the vortices has been illustrated by considering the limiting case of zero included angle between the wing segments at the end of the clap motion. In this case, the circulation Γ^* is large, even though the leading edges of the wing segments have zero velocity.

At a small value of angle of attack ($\alpha = 15$ deg), the circulation may be as high as $\Gamma^* \sim 2$. This much larger value of circulation can be generated at values of reduced frequency a factor of five lower than those employed at zero angle of attack.

Dynamic hysteresis, whereby the flow structure is different at the same angle of attack during the upstroke and downstroke motion, is strikingly evident at finite angle of attack. Whereas substantial circulation Γ^* is generated during the downstroke, negligible Γ^* occurs during the upstroke due to the cancellation effect between the mean angle of attack and the effective angle of attack induced at the leading edge of the wing segment.

Acknowledgments

The authors are grateful to the Air Force Office of Scientific Research for support of this investigation. Professor Stanley Johnson of Lehigh University provided valuable guidance during design of the wing forcing system. Appreciation is also extended to Dr. Geoffrey Spedding of the University of Southern California for insightful comments on this manuscript.

References

[1]Lamar, J. E., "Subsonic Vortex-Flow Design Study of Slender Wings," *Journal of Aircraft,* Vol. 15, Sept. 1978, pp. 611–617.

[2]Lamar, J. E. and Campbell, J. F., "Vortex Flaps–Advanced Control Devices for Supercruise Fighters," *Aerospace America,* Jan. 1984, pp. 95–99.

[3]Rao, D. M., "Leading-Edge Vortex Flaps for Enhanced Subsonic Aerodynamics of Slender Wings," International Council for the Aeronautical Sciences Paper 80-13.5, Oct. 1980.

[4]Rao, D. M., "Upper Vortex Flap–a Versatile Surface for Highly Swept Wings," International Council for the Aeronautical Sciences Paper 82-6.7.1, Aug. 1982.

[5]Rao, D. M., "Segmented Vortex Flaps," AIAA Paper 83-0424, Jan. 1982.

[6]Weis-Fogh, T., "Quick Estimates of Flight Fitness in Hovering Animals, Including Novel Mechanisms for Lift Production," *Journal of Experimental Biology,* Vol. 59, 1973, pp. 160–230.

[7]Maxworthy, T., "Experiments on the Weis-Fogh Mechanism of Lift Production by Insects and Hovering Flight. Part 1: Dynamics of the Fling," *Journal of Fluid Mechanics,* Vol. 93, 1979, pp. 47–63.

[8]Spedding, G. R. and Maxworthy, T., "The Generation of Circulation and Lift in a Rigid Two-Dimensional Fling," *Journal of Fluid Mechanics,* Vol. 165, 1986, pp. 247–272.

[9]Spedding, G. R., Waxworthy, T., and Rignot, E., "Unsteady Vortex Flows over Delta Wings," *Proceedings of Second AFOSR Workshop on Unsteady and Separated Flows,* 1987 (to be published).

[10]Utsch, T. F., "Flow Structure Generation by Segmented Delta Wings Undergoing Controlled Rolling Oscillations," M.S. Thesis, Department of Mechanical Engineering and Mechanics, Lehigh University, Bethlehem, PA, 1987.